Magnetic Field Effects on the Copolymerization of Water-Soluble and Ionic Monomers

IGNACIO RINTOUL,[1] CHRISTINE WANDREY[2]

[1]Facultad de Ingeniería Química, Universidad Nacional del Litoral, Santiago del Estero 2654, CP-3000 Santa Fe, Argentina

[2]Laboratoire de Médecine Régénérative et de Pharmacobiologie, Ecole Polytechnique Fédérale de Lausanne, CH-1015 Lausanne, Suisse

Received 27 June 2008; accepted 13 October 2008
DOI: 10.1002/pola.23152
Published online in Wiley InterScience (www.interscience.wiley.com).

ABSTRACT: The effect of magnetic field (MF) on the radical copolymerization of a series of water-soluble and ionic monomers is presented including acrylamide (AM), acrylic acid (AA), its ionized form acrylate (A^-), and diallyldimethylammonium chloride (DADMAC). The following combinations have been studied: AM/AA, AM/A^-, AM/DADMAC, and AA/DADMAC. In addition to the MF, strong electrostatic interactions are present for the majority of monomer combinations and conditions. Although the monomer consumption rate (R_p) increased up to 65% applying a MF of 0.1 Tesla, the composition of the resulting copolymers was not affected under such conditions. Despite this increase of R_p by MF, the electrostatic repulsion between ionic monomers and charged growing radicals dominates R_p and governs the copolymer composition with and without MF. The order of the experimentally obtained reactivity ratios reflects the extent of electrostatic interaction: $r_{AM/AA}$ (1.41) < r_{AM/A^-} (3.10) < $r_{AA/DADMAC}$ (4.25) < $r_{AM/DADMAC}$ (6.95) and $r_{AA/AM}$ (2.20) > $r_{DADMAC/AA}$ (0.25) > $r_{A^-/AM}$ (0.17) > $r_{DADMAC/AM}$ (0.03). Overall, weak MF offers to reduce the production time without modifying the product composition. © 2008 Wiley Periodicals, Inc. J Polym Sci Part A: Polym Chem 47: 373–383, 2009

Keywords: copolymerization; magnetic field; photopolymerization; reactivity ratios; water-soluble polymers

INTRODUCTION

Water-soluble and ionic copolymers are extensively used in industry, agriculture, and food production. Moreover, a multitude of potential applications in pharmacy and medicine are currently under development. Generally, such copolymers are synthesized through free radical copolymerization, an established procedure to modify polymer properties by arranging different monomer units in a polymer molecule. Free radical copolymerization has a number of advantages due to the versatility, applicability to many functional groups, certain tolerance to impurities, and practicability in both polar and non-polar media. The performance of such polymers for a specific application will depend on their constitution, configuration, and conformation. The growing demand of customized well-defined polymeric architectures has been identified as one of the driving forces for the renaissance of the scientific and technological interest in both, synthetic possibilities and

Correspondence to: I. Rintoul (E-mail: irintoul@santafe-conicet.gov.ar).

mechanistic understanding of free radical copolymerization.[1]

Magnetic field (MF) effects can offer a novel way to modify radical processes. MF has potential advantages over conventional strategies to control free radical copolymerization. Non-contact, instantaneous, homogeneous and highly specific interactions with targeted molecules can be mentioned as examples. In addition, MF interactions may be performed without interfering classical mass and heat transfer processes. MF effects have been observed during the homopolymerization of styrene,[1–9] methyl methacrylate,[10–15] and acrylamide (AM).[10,16] In general, MF increases the efficiency of photoinitiators. In some cases, higher molar mass of the resulting polymers was reported.[7,15,16] Such effects are explained in terms of the radical pair mechanism, which was comprehensively discussed in the review articles of Turro and coworkers[17] and Steiner and Ulrich.[18] MF effects on radical homopolymerizations have been observed and have received proper theoretical analysis. Contrarily, the literature dealing with MF effects on copolymerization reactions is rather limited and reports controversial findings. Only two works describing the influence of MF on reactivity ratios have been found. On the one hand, it was found that acrylonitrile-styrene copolymers synthesized under MF presented higher content of acrylonitrile than copolymers synthesized without MF. In addition, the reactivity ratios of acrylonitrile and styrene were increased and decreased, respectively.[19] On the other hand, no MF effect on the reactivity ratios of AM and acrylic acid (AA) at pH = 3.77 was observed.[20]

This contribution presents a study of the MF effects on the radical copolymerization of four combinations of neutral, anionic, and cationic water-soluble comonomers of high industrial and scientific interest. AM, AA, its ionized species acrylate (A^-), and diallyldimethylammonium chloride (DADMAC) were selected as neutral, anionic, and cationic comonomers. As to the authors' knowledge, the copolymerization of DADMAC with AA is reported for the first time.

A number of researchers have investigated the combinations AM/AA, AM/A^- and AM/DADMAC under various conditions. Because of the technical importance of these copolymers, the interest in research has not diminished for more than 50 years. Table 1 summarizes reactivity ratios of AM/AA, AM/A^-, and AM/DADMAC published by several authors for solution copolymerizations. No data was available for the AA/DADMAC system.

EXPERIMENTAL

Materials

Four times recrystallized AM, (AppliChem, Switzerland), ultra pure AA (BASF, Germany), and a 65 wt % aqueous solution of DADMAC (Sigma-Aldrich, Germany) were used as monomers. Caution: AM is toxic in contact with skin and inhalation and may cause genetic damage. Phenylbis(2,4,6-trimethylbenzoyl)-phosphine oxide, $C_{26}H_{27}O_3P$, dispersed in water (Ciba Specialty Chemicals, Switzerland) served as photoinitiator. The water was of Millipore quality with 18.2 MΩ/cm of resistivity. Ethylene glycol 99% for synthesis (EG), HCl or NaOH, and HPLC grade acetonitrile and methanol (all Apply Chem, Switzerland) were used to adjust the viscosity and the pH of the polymerization medium, and for residual monomer analysis, respectively.

Polymerization Conditions

Syntheses were performed in a 100 mL glass reactor. The reactor was equipped with stirrer, condenser, gas inlet, heating/cooling jacket, and a UV lamp. The temperature was adjusted within ±1 K. The UV lamp had a primary output at $\lambda = 254$ nm with an intensity $I_{UV} = 540$ erg/s cm^2 at the surface of the lamp. The entire reactor was placed between the poles of an electromagnet with maximum 2 Tesla (Bruker-EPRM, Germany).

Oxygen was removed from the initial comonomer solution before the polymerization by purging with N_2 during 30 min at 293 K. Afterward, the temperature was increased to 313 K and the UV lamp was lighted to activate the photodecomposition of $C_{26}H_{27}O_3P$ and to initiate the polymerizations, which were performed isothermally at 313 K and during 60 min. Simultaneously, the MF was adjusted to 0.1 Tesla. Complementary experiments were carried out without MF but keeping constant all other conditions.

Table 2 summarizes the experimental conditions for all AM/AA, AM/A^-, AM/DADMAC, and AA/DADMAC copolymerizations. The polymerization conditions were selected aiming a sufficient linear range of the conversion-time curves. Water/EG mixture (50 wt %; dynamic viscosity $\eta = 10.3 \times 10^{-3}$ Pa s at 313 K) was used as viscous solvent to enhance the MF effect.[31] All polymerizations were performed under pH control. Samples of 0.1–0.2 g were withdrawn from the reactor every 5 min for conversion analysis. Linear conversion-

DOI: 10.1002/pola

Table 1. Reactivity Ratios Published for AM/AA, AM/A$^-$, and AM/DADMAC Copolymerizations

Reactivity Ratios		Polymerization Conditions				
$r_{AM/AA}$	$r_{AA/AM}$	T (K)	[AM] + [AA][a]	M_{AM}[b]	pH	References
0.54	1.48	313	0.40	0.12–0.88	1.80	21
0.50	0.79	333	1.00	0.55–0.97	2.50	22
0.57	1.45	313	1.00	0.75–0.92	1.80	23
0.25	0.92	303	1.00	0.10–0.90	2.10	24
0.48	1.73	333	0.10	0.20–0.80	2.17	25
0.60	1.43	298	1.00	0.12–0.88	1.80	26
r_{AM/A^-}	$r_{A^-/AM}$		[AM] + [A$^-$][a]			
3.04	0.32	313	0.40	0.12–0.88	11.70	21
0.95	0.33	303	1.00	0.10–0.90	9.00	24
1.10	0.35	303	1.00	0.12–0.88	10.00	26
$r_{AM/DADMAC}$	$r_{DADMAC/AM}$		[AM] + [DADMAC][a]			
7.14	0.220	308	4.00	0.20–0.72		27
6.62	0.074	308	3.00	0.11–0.89		27
6.70	0.580	313	1.50	0.10–0.88		28
6.20	0.120	313	2.00	0.50–0.70		29
4.80	0.040	328	3.00	0.43–0.99		30
6.20	0.030	328	1.50	0.10–0.99		30
6.30	0.030	328	0.50	0.10–0.99		30

[a] Concentrations in mol/L.
[b] Acrylamide molar comonomer fraction in the monomer feed.

time curves with $r^2 > 0.99$ were obtained up to at least 10% conversion. Only the linear part of the conversion curves was evaluated for kinetic analysis. Depending on the experimental conditions and the monomer type, the final monomer conversion was between about 10 and 80%.

Analytics and Determination of Copolymer Compositions and Reactivity Ratios

Before analysis, the withdrawn samples were mixed with 5 mL of methanol in the case of AM/AA and AM/A$^-$, or with 5 mL of acetonitrile in the case of AM/DADMAC and AA/DADMAC, to precipitate and isolate the polymer from the solution. The monomers remained in solution. Twenty microliter of the supernatant were injected for HPLC analysis.

The conversion of the copolymerization process was calculated from residual monomer concentration data according to a recently published procedure.[21] The residual monomer concentrations in the withdrawn samples were obtained using a HPLC system composed of a L-6000 Hitachi pump (Hitachi, Japan) and a L-4000H Hitachi UV detector (Hitachi, Japan) operating at 190 nm. The stationary and mobile phases were Nova-Pak (Waters USA) and 5 wt % acetonitrile aqueous solution with a flow rate of 2 mL/min, respectively. The pH of the mobile phase was adjusted to 3.00 with *o*-phosphoric acid to avoid the ionization of AA, which could cause precipitation in the presence of DADMAC.

The HPLC system was calibrated using AM, AA and DADMAC solutions in the concentration range of 7×10^{-4} to 4.5×10^{-3} mol/L. The standard solutions were prepared by sequential dilution of 1 mol/L stock solutions of AM, AA, and DADMAC. The peak area served as calibration parameter. Figure 1 shows typical HPLC calibration curves, with $r^2 \geq 0.999$.

The mathematical procedure to determine the copolymer composition from residual monomer concentration data was described elsewhere in detail.[21] The values of the copolymerization reactivity ratios depend on the treatment of copolymer-comonomer composition raw data. A list of different methods to calculate reactivity ratios was presented in ref. 32. Herein, the calculation of reactivity ratios was carried out using the Tidwell and Mortimer non-linear least squares (NLLS) fitting method.[33,34] The method is based

Table 2. Experimental Conditions of the Copolymerization Series AM/AA, AM/A^-, AM/DADMAC, and AA/DADMAC, Initial Total Comonomer Concentration 0.4 mol/L, $T = 313$ K, $[C_{26}H_{27}O_3P] = 1.2 \times 10^{-3}$ mol/L, and Solvent: 50 wt % Water/EG

		Series 1, AM/AA		Series 2, AM/A^-		Series 3, AM/DADMAC		Series 4, AA/DADMAC	
No.	MF, Tesla	M_{AM}[a]	pH	M_{AM}[a]	pH	M_{AM}[a]	pH	M_{AA}[a]	pH
1	0	0.125	1.75	0.126	11.71	0.129	6.47	0.126	1.82
2	0	0.250	1.87	0.251	11.82	0.251	6.47	0.250	1.76
3	0	0.375	1.94	0.375	11.79	0.375	6.25	0.375	1.79
4	0	0.500	1.93	0.501	11.66	0.500	6.40	0.503	1.83
5	0	0.625	1.93	0.625	11.79	0.625	6.20	0.623	1.91
6	0	0.750	1.92	0.748	11.65	0.748	6.30	0.747	1.86
7	0	0.874	1.93	0.875	11.98	0.869	6.20	0.869	1.92
8	0.1	0.125	1.93	0.125	11.98	0.125	6.51	0.125	1.82
9	0.1	0.251	1.90	0.323	11.67	0.250	6.49	0.245	1.82
10	0.1	0.376	1.92	0.375	11.86	0.371	6.52	0.375	1.79
11	0.1	0.501	1.93	0.499	11.74	0.492	6.50	0.500	1.75
12	0.1	0.625	1.90	0.625	11.67	0.625	6.46	0.625	1.90
13	0.1	0.750	1.92	0.750	11.66	0.748	6.52	0.748	1.85
14	0.1	0.875	1.93	0.874	11.79	0.875	6.32	0.875	1.90

[a] M_{AM} and M_{AA} indicate the molar fractions of AM and AA in the comonomer feed.

on minimizing the sum of squares of weighted residuals [SS ($r_{A/B}$, $r_{B/A}$)] in so-called sum of squares space (SSS) to obtain the most probable set of reactivity ratios, which corresponds to the minimum $ss(r_{A/B}, r_{B/A})$ element. Seven data points were used for the calculation of each of the $ss(r_{A/B}, r_{B/A})$ elements and the weighting factor for each data point was obtained through the assumption of constant relative error. The determination of the joint confidence intervals (JCI) were performed by the so-called *F*-test where the probability *F*-values were used at level $z = 0.90$, that is, 90% probability.[35]

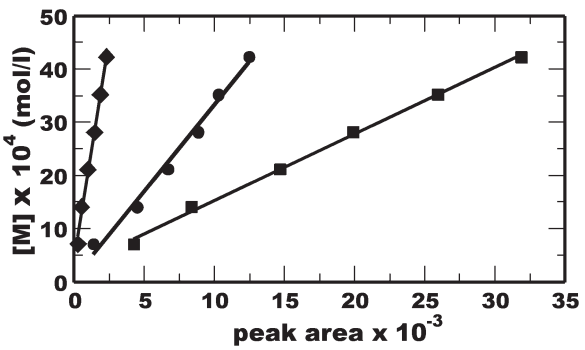

Figure 1. HPLC calibration curves. Concentrations of AM (■), AA (●), and DADMAC (◆) solutions were plotted as a function of the corresponding HPLC peak area.

RESULTS AND DISCUSSION

Conversion Analysis

Figure 2 presents, exemplary, the experimental conversion analysis for AM/A^- copolymerizations at pH = 12. For better visualization, only four monomer ratios have been selected out of seven studied under these reaction conditions.

The continuous, but different, consumption of both monomers is clearly visible. At pH = 12, whatever the monomer ratio is, it is obvious that AM is consumed much faster than A^-. The copolymerization raw data sets of all 56 copolymerizations listed in Table 2 were appropriately evaluated to obtain the monomer consumption rates ($R_p = -d[M]/dt$). This is different from the total polymerization rate defined as $-d[M_1 + M_2]/dt$, which was not considered in this article.

Monomer Consumption Rate

Comparing the copolymerizations performed with and without MF, considerable increase of R_p was observed when the polymerizations were carried out in the presence of MF. Figure 3(a–d) present logarithmic plots of R_p versus [M], where [M] is the concentration of the corresponding comonomers. R_p^{AM}, R_p^{AA}, R_p^{A-}, and R_p^{DADMAC} indicate the monomer consumption rates of AM, AA, A^-, and

DOI: 10.1002/pola

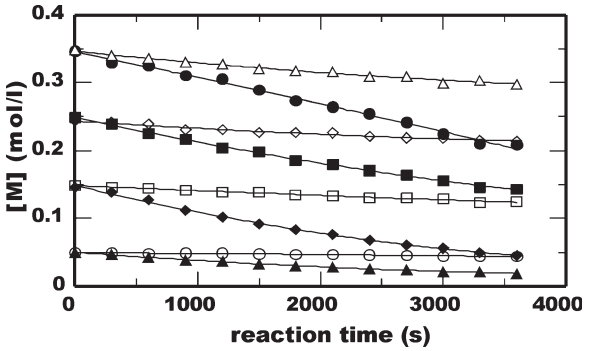

Figure 2. Conversion analysis. Residual monomer concentration ([M]) versus reaction time curves. Residual [AM] (full symbols) and [A^-] (open symbols) of polymerizations with various comonomer ratios (AM/A^-) are plotted as a function of the reaction time. AM/A^- = 7.00 ([●,○), 1.67 (■,□), 0.60 (◆,◇), and 0.14 (▲,△); T = 313 K; pH = 12; [AM] + [A^-] = 0.4 mol/L; [$C_{26}H_{27}O_3P$] = 1.2 × 10^{-3} mol/L; solvent 50 wt % of EG in water; all copolymerizations without MF.

DADMAC during the copolymerization reactions. The values for selected monomer concentrations are summarized in Table 3.

Series 1 in Figure 3(a): AA polymerizes slightly faster than AM at pH = 2. As an example, for [AM] = [AA] = 0.20 mol/L it is R_p^{AA} = 6.58 × 10^{-5} L/mol s, that is higher than R_p^{AM} = 5.01 × 10^{-5} L/mol s. In addition, R_p^{AM} and R_p^{AA} increase with the initial monomer concentration with and without MF. Moreover, R_p^{AM} and R_p^{AA} increased about 60% for all polymerizations when MF was applied.

Series 2 in Figure 3(b): Increasing the pH from 2 to 12 converts AA into A^- and the consumption of AM becomes much faster than the A^- consumption. Specifically, for [AM] = [A^-] = 0.20 mol/L, R_p^{AM} = 2.10 × 10^{-5} L/mol s is about three times higher than R_p^{A-} = 0.66 × 10^{-5} L/mol s when the polymerizations were performed without MF. Interestingly, the MF of 0.1 Tesla increased R_p to R_p^{AM} = 3.23 × 10^{-5} L/mol s and R_p^{A-} = 0.97 × 10^{-5} L/mol s, what is an increase similar to that of AM/AA. Table 3 may be used for further detailed comparison of the kinetic data.

Figure 3(a,b) present the same monomer combination with only modified pH conditions causing either the complete neutralization of AA at pH = 2 or its complete ionization at pH = 12.

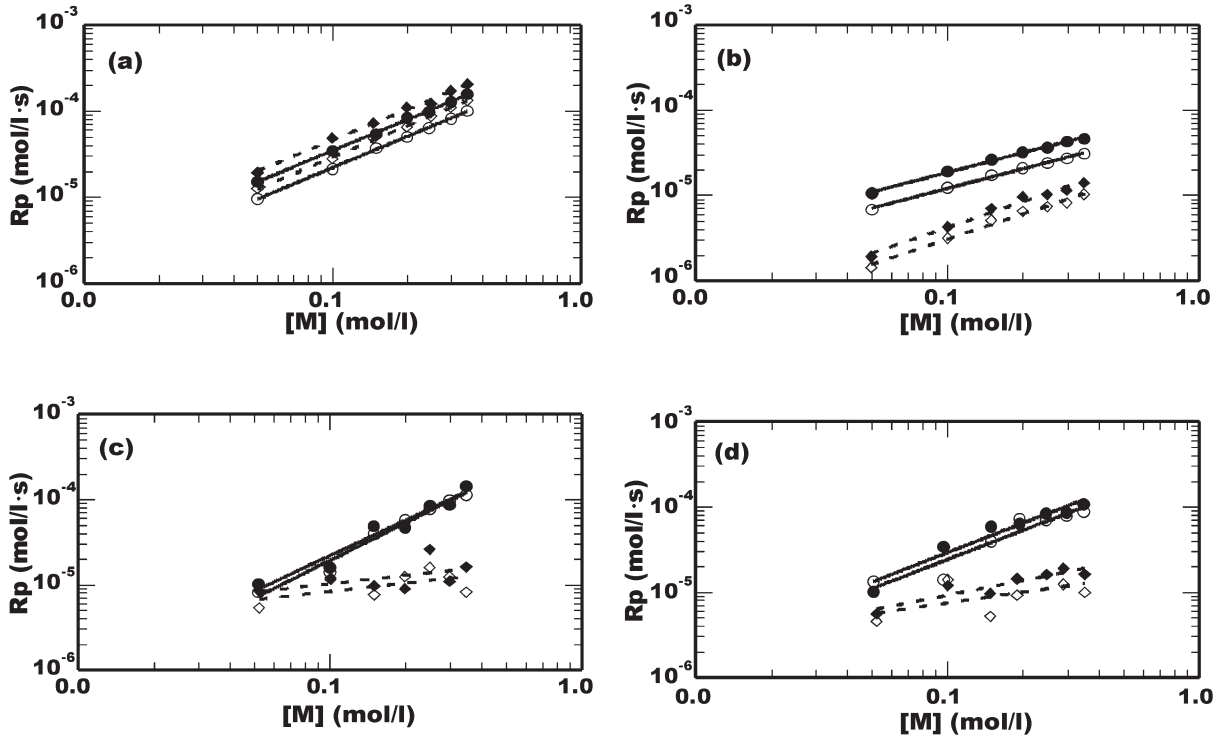

Figure 3. Monomer consumption rates (R_p) versus initial monomer concentrations ([M_1], [M_2]) for copolymerizations with MF (full symbols) and without MF (empty symbols). [$C_{26}H_{27}O_3P$] = 1.2 × 10^{-3} mol/L; T = 313 K; solvent: 50 wt % EG in water; MF = 0.1 Tesla. (a) AM (—, ●,○) and AA (---, ◆,◇) at pH = 2; (b) AM (—, ●,○) and A^- (---, ◆,◇) at pH = 12; (c) AM (—, ●,○) and DADMAC (---, ◆,◇) at pH = 6; and (d) AA (—, ●,○) and DADMAC (---, ◆,◇) at pH = 2; [M_1] + [M_2] = 0.4 mol/L.

Table 3. Monomer Consumption Rates (R_p) of AM, AA, A^-, and DADMAC for their Lowest, Medium and Highest Concentrations in Series 1–4 of Table 2

		$R_p \times 10^5$ L/mol s							
Monomers		Series 1		Series 2		Series 3		Series 4	
[M], mol/L	MF, Tesla	AM	AA	AM	A^-	AM	DADMAC	AA	DADMAC
0.05	0	0.97	1.26	0.69	0.14	0.82	0.54	1.36	0.46
	0.1	1.52	1.94	1.06	0.19	1.04	0.84	1.04	0.56
0.20	0	5.01	6.58	2.10	0.66	5.78	0.77	7.44	0.93
	0.1	8.35	11.04	3.23	0.97	4.69	0.91	6.47	1.44
0.35	0	10.13	13.37	3.12	1.03	11.31	1.24	9.00	1.00
	0.1	15.73	20.55	4.69	1.41	14.50	1.62	11.00	1.62

Comparing the results for AM at pH = 2 (Series 1) and 12 (Series 2), it can be concluded that the AM consumptions decrease while increasing the pH. In fact, comparing the results for [AM] = 0.05 and 0.35 mol/L of these two series, R_p^{AM} was obtained as 0.97×10^{-5} and 10.13×10^{-5} L/mol s at pH = 2 but as 0.69×10^{-5} and 3.12×10^{-5} L/mol s at pH = 12. However the impact of the pH is much stronger on acrylic acid comparing the same concentrations. R_p^{AA} (pH = 2) was found about 9–13 times higher than R_p^{A-} (pH = 12). Same trends hold for polymerizations under MF.

Figure 3(c,d) present R_p^{AM}, R_p^{AA}, and R_p^{DADMAC} as a function of [AM], [AA], and [DADMAC] in the comonomer feed during their copolymerization with and without MF. The results reveal higher fluctuations than visible from Figure 3(a,b), especially for R_p^{DADMAC}. Such experimental scatter is due to the considerably higher slope of the DADMAC calibration curve in Figure 1 compared with AM and AA. Therefore, significant variations of [DADMAC] are monitored by only small changes in the peak areas during HPLC analysis preventing high precision of the conversion curves. Subsequently, less accuracy of the conversion curves is propagated to the R_p values. Despite the lower precision, general trends may be concluded.

R_p^{AM} of Series 3 in Figure 3(c) presents almost the same values as R_p^{AM} of Series 1 in Figure 3(a). Therefore, the polymerization of AM as copolymerization component seems neither to be affected by increasing the pH from 2 to 6, nor by exchanging the neutral AA by the cationic DADMAC comonomer. However, R_p^{AM} is significantly decreased at pH = 12 and in the presence of the anionic A^- comonomer. Specifically, for Series 3 where DADMAC was present, R_p^{AM} increased from 0.82×10^{-5} to 11.31×10^{-5} L/mol s when [AM] was varied from 0.05 to 0.35 mol/L in the comonomer feed, whereas the increase was only from 0.69×10^{-5} L/mol s to 3.12×10^{-5} L/mol s in presence of A^- at pH = 12. MF effect could not undoubtedly be assigned to AM and DADMAC in Series 3, as well as AA and DADMAC in Series 4, due to the analytical uncertainty discussed above. Surprisingly, R_p^{DADMAC} in Figure 3(c,d) seems to be less sensitive to [M] in this range than R_p^{A-} in Figure 3(b), both corresponding to fully ionized monomers.

Table 4 summarizes the concentration dependence of all monomer consumptions as slope of the appropriate curves in Figure 3(a–d). Despite absolutely higher R_p values, no influence of the MF on the concentration dependence can be concluded within the range of experimental error.

Table 4. Slopes of the Logarithmic Plots $R_p = f([M])$ in Figure 3(a–d)

		Slopes for MF = 0			Slopes for MF = 0.1 Tesla		
Series	pH	AM	AA/A^-	DADMAC	AM	AA/A^-	DADMAC
1	2	1.20	1.21	–	1.20	1.19	–
2	12	0.77	0.98	–	0.76	1.01	–
3	6	1.38	–	0.32	1.48	–	0.33
4	2	–	1.14	0.42	–	1.15	0.58

DOI: 10.1002/pola

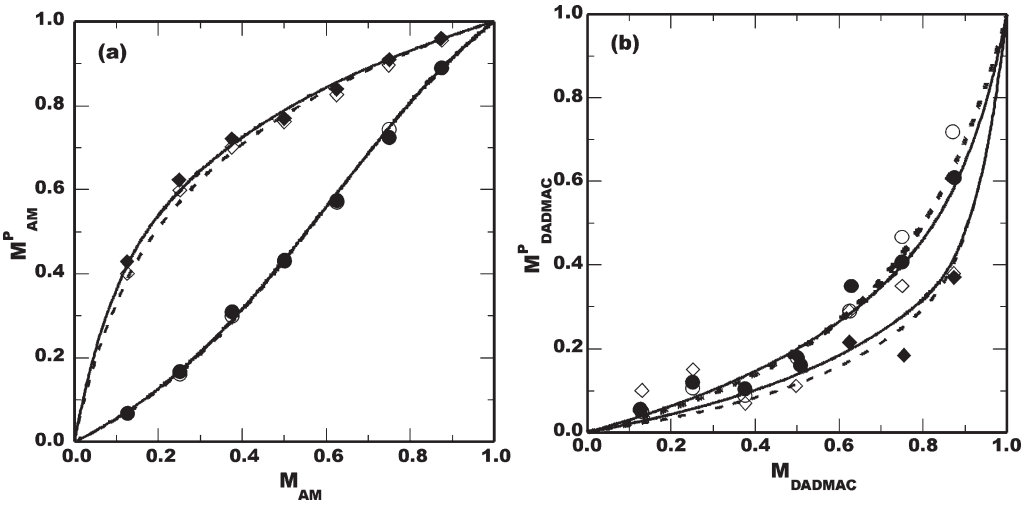

Figure 4. Copolymerization diagrams for copolymerizations carried out with MF (full symbols) and without MF (empty symbols). $[C_{26}H_{27}O_3P] = 1.2 \times 10^{-3}$ mol/L; T = 313 K; solvent: 50 wt % of EG in water; MF = 0.1 Tesla. (a) AM/AA at pH = 2 (●,○) and AM/A^- at pH = 12 (◆,◇). (b) AM/DADMAC at pH = 6 (◆,◇) and AA/DADMAC at pH = 2 (●,○). Curves calculated using the reactivity ratios of Table 5: with MF (–), without MF (---).

Copolymer Composition and Reactivity Ratios

Based on the conversion analysis data, copolymerization diagrams were constructed. The diagrams are presented in Figure 4(a), for Series 1 and 2, and in Figure 4(b), for Series 3 and 4.

Figure 4(a) reveals differences of the copolymer composition for copolymers obtained from the same monomer feed mixtures but from copolymerizations performed at different pH. Copolymers synthesized at pH = 2 yielded approximately the same composition as mixed in the comonomer feed, whereas copolymers synthesized at pH = 12 resulted enriched in AM units. AM/DADMAC and AA/DADMAC yielded copolymers enriched with AM or AA units compared with the corresponding feed composition as visualized in Figure 4(b). However, neither for Series 1 and 2 nor for Series 3 and 4, MF effects can undoubtedly be concluded.

The NLLS fitting method was used and the 90% joint confidence intervals were constructed as presented in Figure 5(a–d). Table 5 summarizes the reactivity ratios.

The reactivity ratios presented in Table 5 reflect the preferred polymerization of AM for Series 2 and 3, and of AA for Series 4. Here, $r_{\text{AM (or AA)/comonomer}}$ is significantly higher than $r_{\text{comonomer/AM (or AA)}}$. For Series 1, the reactivity ratios of AM and AA differ less. The overlapping JCIs in Figure 5(a–d) and the values in Table 5 confirm that the reactivity ratios for all copolymerizations cannot be considered as affected by the MF, though slightly lower values were calculated for the majority of cases where MF was applied.

It is visible that the contours of the confidence intervals in Figure 5(c,d) extend into the negative range and include zero. This is a consequence of the arbitrary requirement for 90% confidence and the relatively low values of $r_{\text{DADMAC/comonomer}}$. Mathematically, the confidence intervals close in the negative region passing through zero. Negative regions are not presented herein due to their physical impossiblity. As the probability of homo and crosspropagation is always >0, the reactivity ratios will be $r_{i\text{-}j} > 0$ and $r_{j\text{-}i} > 0$. This justifies the plots only in the first quadrant. Negative values are an intrinsic result of the statistics and depend on the percentage of confidence arbitrarily set. Reduction of confidence will reduce the area of the ellipsoids whereas increasing the percentage would result in extension of the intervals of all reactivity ratios.

Comparison of Experimental Results and Literature Data

When comparing the experimental results summarized in Table 5 with the literature data of Table 1 one has to consider that all copolymerizations of this study were performed in a medium of enhanced initial viscosity, 50 wt % of EG in water. Actually, the viscosity of the EG/water mixture was

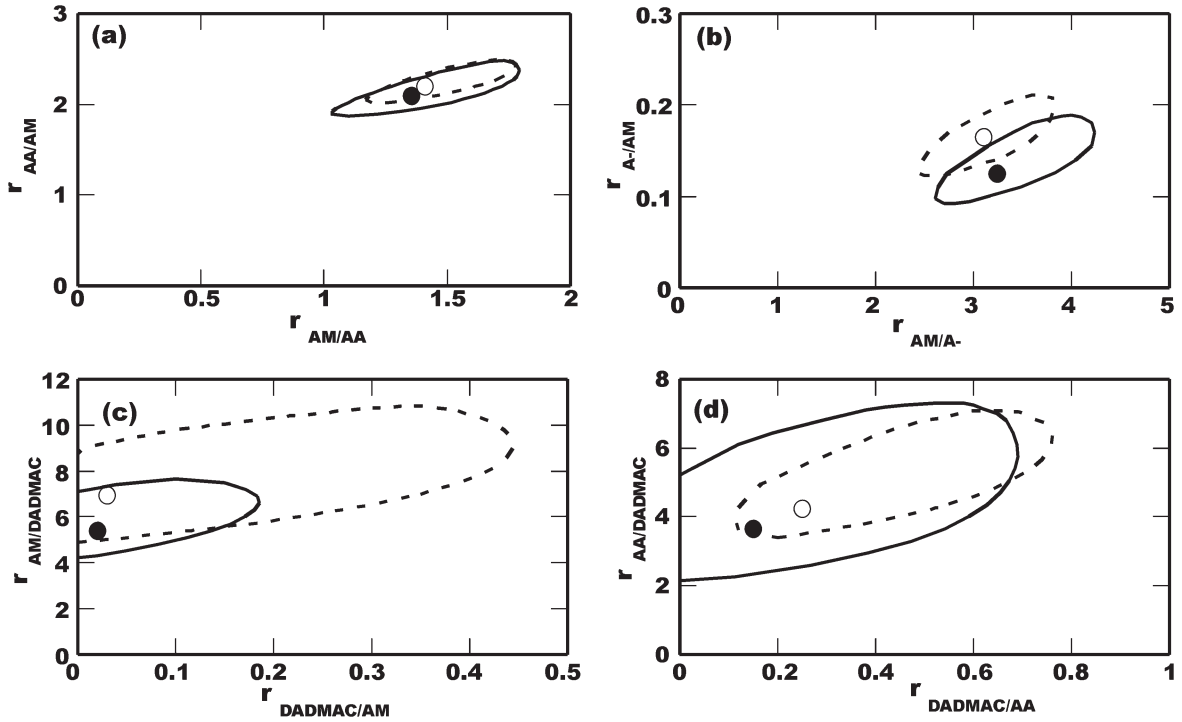

Figure 5. Determination of reactivity ratios. Copolymerizations carried out with MF (●) and without MF (○). $[C_{26}H_{27}O_3P] = 1.2 \times 10^{-3}$ mol/L; $T = 313$ K; solvent: 50 wt % EG in water; MF = 0.1 Tesla. (a) AM/AA at pH = 2; (b) AM/A^- at pH = 12; (c) AM/DADMAC at pH = 6; (d) AA/DADMAC at pH = 2; JCI with MF (–) without MF (---).

10.3×10^{-3} Pa s instead of 5×10^{-3} Pa s in pure water. Moreover, also the total monomer concentration, polymerization temperature, pH, and the AM molar comonomer fraction in the monomer feed, and the method to calculate the reactivity ratios, were differently chosen by other authors.

Nevertheless, all authors report $r_{AM/AA} < r_{AA/AM}$ what is in agreement with the results of Series 1 in Table 5. Differently, herein $r_{AM/AA}$ and $r_{AA/AM}$ were both found >1, with and without MF. This refers to an azeotrop copolymerization behavior. Such azeotrop copolymerization can be concluded from other studies listed in Table 1[22,24] where both $r_{AM/AA}$ and $r_{AA/AM}$ were <1. Overall, the trends reported in Table 1, $r_{AM/A^-} \gg r_{A^-/AM}$ and $r_{AM/DADMAC} \gg r_{DADMAC/AM}$, are confirmed by the reactivity ratios in Table 5 for polymerizations with and without MF. No comparison can be made for Series 4. This monomer combination was studied for the first time here.

Table 5. Reactivity Ratios for the Copolymerization of AM/AA, AM/A^-, AM/DADMAC, and AA/DADMAC, $[C_{26}H_{27}O_3P] = 1.2 \times 10^{-3}$ mol/L, $T = 313$ K, Solvent: 50 wt % EG in Water, and MF = 0.1 Tesla

		Tidwell-Mortimer	
Series	Reactivity Ratios	Without MF	With MF
1	$r_{AM/AA}$	1.41	1.36
	$r_{AA/AM}$	2.20	2.10
2	r_{AM/A^-}	3.10	3.24
	$r_{A^-/AM}$	0.17	0.13
3	$r_{AM/DADMAC}$	6.95	5.40
	$r_{DADMAC/AM}$	0.03	0.02
4	$r_{AA/DADMAC}$	4.25	3.65
	$r_{DADMAC/AA}$	0.25	0.15

Electrostatic Interactions

Strong influence of the pH on the polymerization rate is clearly visible comparing Figure 3(a,b). The main impact is expected from the degree of ionization of AA monomers and polymer chain units. At pH = 2, both monomers, AM and AA are not ionized and present similar reactivity which indeed depends on the monomer ratio in the feed. The addition of AA is slightly preferred at low AM ratio in the feed, while the situation is inversed at high AM ratio. The model curve in Figure 4(a)

DOI: 10.1002/pola

reflects this behavior. Further influence can be suggested for different total monomer concentrations, but only one total monomer concentration was studied here.

At pH = 12, AM is coexisting with A^-. Here, the repulsive forces due to the negative charges of the A^- monomers as well as the negatively charged A^- chain units of the copolymer molecules dominate over size and polarity effects caused by the amide and acidic groups in AM and AA. In such case, the addition of ionized A^- monomer to a negatively charged growing radical is significantly impaired, especially when the terminal unit of the growing radical is also ionized, such as at pH = 12. Thus, it is expected that a growing radical will preferentially react with AM, and the copolymers become enriched with AM units, which is quantitatively reflected by r_{AM/A^-} (3.10) $\gg r_{A^-/AM}$ (0.17).

A similar situation exists for the copolymerization of AM with DADMAC. However, the differences, r_{AM/A^-} (3.10) $< r_{AM/DADMAC}$ (6.95) and $r_{A^-/AM}$ (0.17) $> r_{DADMAC/AM}$ (0.03), indicate that electrostatic effects are more pronounced for AM/DADMAC. The almost pH independent positive charge in a DADMAC terminal chain unit is very close located to the radical center impairing the approach of DADMAC monomers. Thus, the homopropagation rate coefficient for DADMAC is expected to be lower than the homopropagation rate coefficient for AM and even A^-.

Interestingly, r_{AM/A^-} (3.10) $< r_{AA/DADMAC}$ (4.25) $< r_{AM/DADMAC}$ (6.95) were determined, implying for AA/DADMAC copolymers less composition drift than for AM/DADMAC. Here, the high ionic strength of the polymerization medium seems to suppress, partially, the electrostatic repulsion between the ionic monomer and growing radicals. Enhanced ionic strength in the polymerization medium of Series 4 is achieved due to the addition of HCl needed to adjust the low pH = 2. The excess of chloride ions screens the positive charge of the quaternized ammonium allowing DADMAC monomers and growing radicals to approach, and to react, easier than under the conditions of Series 3 where the pH was about 6.5. Therefore, the effect primarily results from the ionic strength induced by pH adjustment.

Influence of Magnetic Field on the Polymerization Rate

Overall, for all copolymerizations performed under MF higher R_p than for copolymerizations without MF were observed [Fig. 3(a–d)]. This effect can be explained in terms of the radical pair mechanism. The photoinitiator used here, $C_{26}H_{27}O_3P$, decomposes yielding two radicals in triplet state trapped in a cage formed by solvent and monomer molecules. When the photodecomposition of $C_{26}H_{27}O_3P$ occurs under classical conditions, that is, in a non-magnetic environment, the three states composing the triplet state (T_+, T_0 and T_-) are equally populated. However, T_0 may pass to the singlet spin state (S) through the so-called Δg mechanism.[4] As soon as a radical pair passes to the S state, the probability to recombine to $C_{26}H_{27}O_3P$ becomes high. Another possibility for reactions in S state is the formation of cage products, which, normally, have lower probability than recombination reactions. However, regenerated $C_{26}H_{27}O_3P$ may decompose again while the formation of cage products results in wastage of initiator.[36]

Without MF, as T_0 passes to S, T_+ and T_- pass to T_0 to maintain the three T states equally populated.[37] Finally, an overall transformation of T into S state with associated regeneration of $C_{26}H_{27}O_3P$ can be concluded. Accidentally, one of the radicals trapped in the cage may react with a monomer molecule, or a solvent molecule may enter in between the radical pair. In such cases, the radicals are released from the cage and are able to initiate polymerization.

When MF is applied, $C_{26}H_{27}O_3P$ decomposes yielding radical pairs exclusively in the T_+ state, which then cannot easily pass to the T_0 state. Consequently, the generation of radical pairs in S state does not occur and thus, recombination reaction and formation of cage products are inhibited. Trapped radicals, quenched in the T_+ state, have higher lifetime, which increases substantially the probability to escape from the cage. Therefore, more radicals are released to the monomer mixture increasing the overall R_p. Furthermore, the termination reaction may be inhibited in a similar way, as it was demonstrated for the homopolymerization of AM with MF.[38]

Another mechanism usable to explain the enhanced monomer consumption in the MF relates to reaction-favorable magnetic orientation of the monomer molecules. It is known that organic molecules, such as the monomers studied here, possess some degree of diamagnetic anisotropy. This property tends to orientate the molecules in the direction of the field depending on the temperature of the system and the MF intensity. Polymerizations of monomers with specific

preferred orientation are faster than polymerizations of randomly oriented monomers systems.[39] Mechanistically, such ordering would increase the propagation rate coefficient. This is a hypothesis suggested as not being the case herein. Molecule orientation has not been reported for MF as low as 0.1 Tesla. Nevertheless, both MF spin effects during the radical generation and termination as well as magnetically induced orientation of monomer molecules influencing the initiation as well as propagation steps of the radical polymerization are hypothesized to explain the increment of R_p with MF.

Influence of Magnetic Field on Copolymer Compositions and Reactivity Ratios

Figure 4(a,b) suggest that the application of MF during the copolymerization of AM/AA, AM/A^-, AM/DADMAC, and AA/DADMAC does not affect the composition of the copolymers. These results support the MF spin effect. As the copolymer composition is basically a function of reactivity ratios, which are defined as the ratios of the homopropagation and cross-propagation rate coefficients, and as reactivity ratios were not affected by MF, it can be concluded that the propagation step of radical polymerizations is not affected by MF or that the homo and cross-propagation rate coefficients are affected to the same extent. The first hypothesis suggests that MF effects belong to other steps of polymerization, that is, initiation and/or termination. The second, and less probable hypothesis, proposes the propagation step to be affected by MF. Propagation may be influenced by MF induced molecular orientation of monomers and growing radicals. However, different species normally have different diamagnetic susceptibilities and thus they respond differently to the same MF intensity. Therefore, homo and cross-propagation rate coefficients can be expected being affected in different manner when MF is applied. Such effect should be evident by changes in the reactivity ratios, which is not the case here. Conclusively, based on the experimental findings, a MF intensity of 0.1 Tesla is suggested to be not strong enough to induce significant monomer orientation, which could turn into an increment of the propagation rate coefficients.

MF interactions through the radical pair mechanism during the generation and termination of radical pairs seem to be the most appropriate mechanism to describe the increment of R_p and the invariability of copolymer composition and reactivity ratios with MF.

CONCLUSIONS

The application of low MF intensity substantially increases the efficiency for radical production of $C_{26}H_{27}O_3P$ when it is photochemically decomposed. Such higher efficiency was explained in terms of the intersystem crossing mechanism between *S*-T spin states. The increase of the efficiency of the photoinitiator yields higher radical concentration in the polymerization medium when MF is applied. Thus, faster monomer consumption is observed. However, the copolymer composition was not affected by MF. Consequently, the homo and crosspropagation rate coefficients were concluded as not influenced by MF = 0.1 Tesla.

Electrostatic interactions between monomers and growing radicals dominate over MF effects. Monomer consumption rate and final copolymer compositions depend much stronger on electrostatic interactions than on MF. Mechanistically, the repulsive forces between equally charged monomers and growing radicals, which impair the approach and subsequent addition of monomers to the growing radical, serve as explanation. As a consequence, the copolymer products are significantly enriched in the non-ionized monomer. Electrostatic effects become more significant for systems with charges located closer to the radical center and diminish with the increase of the ionic strength of the polymerization medium.

Low magnetic fields such as applied herein may serve to optimize time or temperature regimes and productivity of the copolymerization process in a non-contact, homogeneous and instantaneous manner without modifying the product composition, recipe formulations and other conditions related to mass and heat transfer processes.

The authors thank the Swiss National Science Foundation for the financial support (Grants 2000-63,395 and 200020-100250), Ciba Specialties for providing the photoinitiator (Irgacure 819DW), and Dr. Giovanni Boero (Laboratory of MicroSystems, EPFL) for assistance with the electromagnet.

REFERENCES AND NOTES

1. Hawker, C. J.; Bosman, A. W.; Harth, E. Chem Rev 2001, 101, 3661–3688.

2. Turro, N. J.; Chow, M. F.; Chung, C. J.; Tung, C. H. J Am Chem Soc 1980, 102, 7391–7393.
3. Turro, N. J. Ind Eng Chem Prod Res Dev 1983, 22, 272–276.
4. Turro, N. J.; Chow, M. F.; Chung, C. J.; Tung, C. H. J Am Chem Soc 1983, 105, 1572–1577.
5. Huang, J. L.; Song, Q. H. Macromolecules 1993, 26, 1359–1362.
6. Huang, J. L.; Hu, Y. Q.; Song, Q. H. Polymer 1994, 35, 1105–1108.
7. Bag, D. S.; Maiti, S. Polymer 1998, 39, 525–531.
8. Liu, J.; Zhang, R.; Li, H. P.; Han, B. X.; Liu, Z. M.; Jiang, T.; He, J.; Zhang, X. G.; Yang, G. Y. New J Chem 2002, 26, 958–961.
9. Ushakova, M. A.; Chernyshev, A. V.; Taraban, M. B.; Petrov, A. K. Eur Polym J 2003, 39, 2301–2306.
10. Simionescu, C. I.; Chiriac, A.; Neamtu, I. Polym Bull 1991, 27, 31–36.
11. Simionescu, C. I.; Chiriac, A. P.; Chiriac, M. V. Polymer 1993, 34, 3917–3920.
12. Chiriac, A. P.; Simionescu, C. I. J Polym Sci Part A 1996, 34, 567–573.
13. Chiriac, A. P. J Polym Sci Part A 2004, 42, 5678–5686.
14. Chiriac, A. J Appl Polym Sci 2004, 92, 1031–1036.
15. Chiriac, A. P.; Simionescu, C. I. Polym Test 1996, 15, 537–548.
16. Bag, D. S.; Maiti, S. J Polym Sci Part A 1998, 36, 1509–1513.
17. Khudyakov, I. V.; Arsu, N.; Jockusch, S.; Turro, N. J. Desig Monom Polym 2003, 6, 91–101.
18. Steiner, U. E.; Ulrich, T. Chem Rev 1989, 89, 51–147.
19. Bag, D. S.; Maiti, S. Indian J Chem 1998, 37, 212–221.
20. Chiriac, A. P.; Simionescu, C. I. Rev Roum Chim 1997, 42, 743–746.
21. Rintoul, I.; Wandrey, C. Polymer 2005, 46, 4525–4532.
22. Truong, N. D.; Galin, J. C.; Francois, J.; Pham, Q. Polymer 1986, 27, 467–475.
23. Shawki, S. M.; Hamielec, A. E. J Appl Polym Sci 1979, 23, 3155–3166.
24. Ponratnam, S.; Lal Kapur, S. Makromol Chem 1977, 178, 1029–1038.
25. Cabaness, W. R.; Lin, T. Y. C.; Parkanyi, C. J Polym Sci Part A-1 1971, 9, 2155–2170.
26. Bourdais, J. Bull Soc Chim Fr 1955, 93, 485–489.
27. Wandrey, C.; Jaeger, W. Acta Polym 1985, 36, 100–110.
28. Tanaka, H. J Polym Sci Part A 1986, 24, 29–36.
29. Matsumoto, A.; Wakabayashi, S.; Oiwa, M.; Butler, G. B. J Macromol Sci Chem Part A 1989, 26, 1475–1487.
30. Brand, F.; Dautzenberg, H.; Jaeger, W.; Hahn, M. Angew Makromol Chem 1997, 248, 41–71.
31. Vedeneev, A. A.; Khudyakov, I. V.; Golubkova, N. A.; Kuzmin, V. A. J Chem Soc Farad Trans 1990, 86, 3545–3549.
32. Rintoul, I.; Wandrey, C. Macromolecules 2005, 38, 8108–8115.
33. Van Herk, A. M. J Chem Educ 1995, 72, 138–140.
34. Tidwell, P. W.; Mortimer, G. A. J Polym Sci Part A 1965, 3, 369–387.
35. Behnken, D. W. J Polym Sci Part A 1964, 2, 645–650.
36. Kolczak, U.; Rist, G.; Dietliker, K.; Wirz, J. J Am Chem Soc 1996, 118, 6477–6489.
37. Carrington, A.; McLachlan, A. D. In Introduction to Magnetic Resonance with Application to Chemistry and Chem Physics; Harper and Row: New York, 1967, Chapter 1, pp 1–12.
38. Rintoul, I.; Wandrey, C. Polymer 2007, 48, 1903–1914.
39. Chapiro, A.; Dulieu, J. Eur Polym Mater 1977, 13, 563–577.